DSMC-SPARTA implementation of majorant collision frequency scheme

Cite as: AIP Conference Proceedings **2132**, 070026 (2019); https://doi.org/10.1063/1.5119580
Published Online: 05 August 2019

Aaron Pikus, Israel B. Sebastião, Shashank Jaiswal, Michael Gallis, and Alina A. Alexeenko

DSMC-SPARTA Implementation of Majorant Collision Frequency Scheme

Aaron Pikus[1], Israel B. Sebastião[1], Shashank Jaiswal[1], Michael Gallis[2] and Alina A. Alexeenko[1,a)]

[1]*School of Aeronautics and Astronautics, Purdue University (USA)*
[2]*Engineering Sciences Center, Sandia National Laboratories (USA)*

[a)]Corresponding author: alexeenk@purdue.edu

Abstract. The direct simulation Monte Carlo (DSMC) method takes a stochastic approach to solving the Boltzmann equation, and is commonly used to model rarefied gas flows. The simulation domain is split into cells, in which computational representative particles mimic the real flow. Since millions to billions of particles need to be tracked, these models need to be both accurate and computationally efficient. Even with high-fidelity collision models, the overall accuracy of the DSMC outcome strongly depends on its ability to predict the correct number of collision events per simulated time step, i.e. the collision frequency. The two most popular approaches for this purpose are the no-time-counter (NTC) and majorant collision frequency (MCF) schemes. While the NTC scheme is designed to reproduce the average collision time for a sufficiently large sample sizes, the MCF scheme has the advantage of reproducing the exact Poisson distribution of collision time as well as the mean collision time with a reduced sample size. Both schemes have linear complexity of O(N), with N being the number of particles. In this work, we implement the MCF scheme in SPARTA, an open source DSMC solver. A series of numerical tests are performed to illustrate the efficiency and accuracy of both the schemes. Various benchmarks highlighting unsteady, compression, and expansion problems are studied.

INTRODUCTION

The direct simulation Monte Carlo [1] (DSMC) method is a probabilistic technique for modeling rarefied gas flows. The simulation domain is discretized and computational particles are employed to reproduce solve the Boltzmann equation [2]. The algorithm then iterates until the specific simulation time is complete. One key component throughout the iteration process is the collision step, which relies on phenomenological models and collision schemes. Elastic scattering, internal energy relaxation, chemistry, and gas surface interactions are typical molecular processes that are described by the phenomenological models for every collision. Computationally efficient models are required to successfully reproduce macroscopic rates obtained from experimental results. Even when efficient and high fidelity collision models are used, the DSMC calculation will only be accurate with collision schemes that reproduce the correct collision frequency.

Two popular schemes for reproducing the collision frequency are no time counter [1] (NTC), and majorant collision frequency [3] (MCF). NTC was introduced by Bird, and modern solvers like SPARTA [4] use it. MCF was introduced by Ivanov, and is mainly used in SMILE [5]. Previously, both schemes were compared by Venkattraman et al [6]. MCF was implementated in Bird's DSMC0 (0-D) code, and it was determined that MCF reproduces the Poisson distribution (Equation 1) better than NTC given the same conditions. However, it is still unclear, from a practical perspective, if it is beneficial to capture the distribution function of time between collisions, or if the mean collision time (τ) is sufficient.

$$f(t_c) = \frac{1}{\tau} exp(-\frac{t_c}{\tau}) \tag{1}$$

The goal of this work is to implement the MCF scheme in SPARTA and compare it with the NTC scheme. Besides verifying the MCF-SPARTA implementation for 0D cases [6], we also compare NTC and MCF schemes for unsteady and multidimensional nonreactive flows. The remainder of this paper is organized as follows. First, both

31st International Symposium on Rarefied Gas Dynamics
AIP Conf. Proc. 2132, 070026-1–070026-9; https://doi.org/10.1063/1.5119580
Published by AIP Publishing. 978-0-7354-1874-5/$30.00

collision schemes are explained. Then several benchmark cases are discussed and the results of both MCF and NTC are compared.

BACKGROUND

One of the earliest collision schemes was the time counter (TC) scheme [7], where a collision pair is chosen, and the collision is accepted with the probability $((\sigma_T c_r)/(\sigma_T c_r)_{max})$, where σ_T is the total collision cross section for the collision pair, and c_r is the relative speed of the collision pair. A time increment (Δt_c) for the collision is computed as shown in Equation 2.

$$\Delta t_c = \frac{2V}{N\bar{N}F_{NUM}\sigma_T c_r} \tag{2}$$

where V is the cell volume, N is the number of simulators in the collision cell, $\bar{N}$ is its time average, and F_{NUM} is the ratio of real molecules to computational molecules. If the collision is accepted, the post-collision velocities and internal energies are computed. This step is repeated until $\sum t_c \geq \Delta t$. This algorithm is computationally efficient with a O(N) complexity, but the collision scheme fails to reproduce the correct collision frequency under extreme non-equilibrium conditions [8, 9].

Both NTC and MCF have a complexity of O(N) and can reproduce the theoretical mean collision frequency ($\nu = 1/\tau$) for typical numbers of DSMC simulated particles/cell (i.e. ~20), even in extreme non-equilibrium conditions. However, these schemes have a very important difference. With NTC, the solver calculates the number of collisions it will attempt, and then increments until it has tested all possible collisions. With MCF, the algorithm computes the majorant frequency within the collision cell (which is larger than the actual collision frequency), and uses that to compute a secondary timestep δt. Collisions are tested until the sum of the secondary timesteps is greater than the overall simulation timestep. Although NTC reproduces the mean number of collisions, only MCF samples the time between collision from the exact Poisson distribution (Equation 1). Both schemes are summarized in Figure 1.

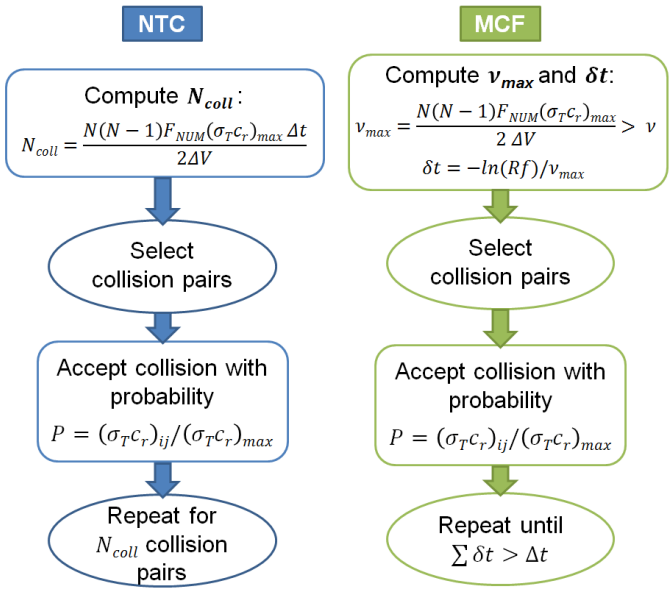

FIGURE 1. Comparison of NTC and MCF collision schemes

Figure 2 shows that under equilibrium conditions, over 85% of all collisions occur within the first $2t_c/\tau$, and about 98% of collisions occur within $4t_c/\tau$. This means that the collision scheme needs to perform well in this time period.

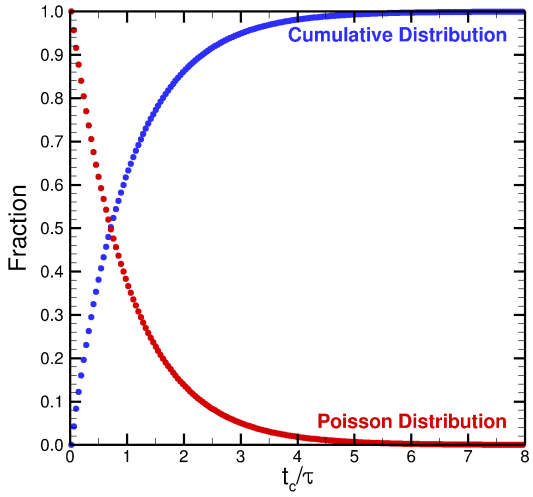

FIGURE 2. Theoretical/Poisson distribution of time between collisions for an equilibrium gas.

Collision Time Sampling

NTC and MCF schemes have a major conceptual difference that should be considered when sampling/binning the time between collisions (Figure 3). In NTC, the minimum binning interval is the simulation timestep (Δt), as that is the minimum time resolution for the collision scheme. Any collision that occurs can only be assigned to that timestep, not an intermediate time. However, MCF has a much smaller time resolution as it calculates a second timestep (δt). This means that the time associated with the collision isn't the timestep itself, but some intermediate time. This means that any binning interval, even one much smaller than the timestep, is suitable for MCF.

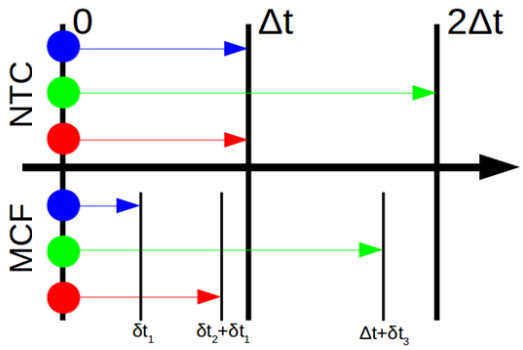

FIGURE 3. Difference in time resolution of NTC and MCF result in different binning. Even though the red and blue particles collide at different times, NTC sees them as colliding at the same time because they collide in the same timestep.

RESULTS

0-D Steady Case

A 0-D homogeneous and adiabatic system was used to verify the MCF implementation, as was done in Venkattraman et al [6]. The time between accepted collisions for MCF and NTC schemes is sampled at a minimum bin size of $1\mu s$ and compared to the Poisson distribution. The numerical and VHS parameters are shown in Table 1, where n is the gas number density, T is the gas temperature, m is the molecular mass, τ_{TH} is the theoretical mean collision time, ω

is the viscosity coefficient, and α is the VSS scattering coefficient. Δx is the cell size, which was chosen to be about 1/10th of the mean free path.

Note that the total number of particles (N_P) was kept at 10,000, and the cell size was held at 1 mm for all cases. To vary the number of particles per cell, the domain size was changed in the x-direction. For two particles per cell, the domain was 5.0 m long, while for 100 particles per cell, the domain was 0.1 m long. We also increased the timestep to see if MCF can reproduce the Poisson distribution with the timestep equal to the mean collision time.

TABLE 1. Investigated numerical and VHS conditions

n [m^{-3}]	1.4x10^{20}
T [K]	273
m [kg]	5.0x10^{26}
N_p [-]*	10,000
Δx_{cell} [mm]*	1
Simulated time [ms]	50
τ_{TH} [μs]	23.5
T_{ref} [K]	273
d_{ref} [m]	4x10^{-10}
ω [-]	1
α [-]	1

* Domain size is adjusted to keep N_p and Δx_{cell} constant.

The simulation ran until around 10 million collisions were accepted (20 million samples). First, the mean collision frequency was sampled from DSMC and compared to the theoretical collision frequency, as shown in Table 2. We can see that both schemes reproduce the mean collision frequency within 0.1%, even for very large timesteps.

TABLE 2. Equilibrium mean collision time for both MCF and NTC. Different timesteps and particles per cell (ppc) are considered

	MCF				**NTC**			
ppc	$\Delta t/\tau_{TH}$	τ/τ_{TH}	$\Delta t/\tau_{TH}$	τ/τ_{TH}	$\Delta t/\tau_{TH}$	τ/τ_{TH}	$\Delta t/\tau_{TH}$	τ/τ_{TH}
2	1/10	0.9995	1	0.9999	1/10	0.9995	1	0.9998
8	1/10	0.9995	1	0.9994	1/10	0.9995	1	0.9996
20	1/10	0.9995	1	0.9993	1/10	0.9995	1	0.9997
100	1/10	0.9995	1	0.9998	1/10	0.9995	1	0.9998

The time between accepted collisions was sampled, and a probability distribution function (PDF) was constructed of 1 μs bins. Figure 4 shows a comparison of the ratio of the PDF calculated from DSMC to the theoretical Poisson distribution for different number of particles and timesteps for MCF and NTC. We can see that for a reasonable timestep of $\Delta t/\tau = 10$, MCF reproduces the Poisson distribution better than NTC with eight or more particles per cell. Even with a very large timestep however, MCF can still reproduce the Poisson distribution well with 20 particles per cell. Note that NTC effectively has fewer bins for a timestep that is larger than the bin size, as discussed in Figure 3.

We can conclude that MCF can reproduce the distribution of collisions well even for large timesteps. Next, we look to investigate certain applications where MCF might be computationally beneficial, as it might allow for fewer particles per cell or a larger timestep.

1D Oscillatory Couette Flow

A 1-D oscillatory coutte flow [10] was chosen to compare the computational performance of NTC and MCF for unsteady flows. We varied the timestep and number of particles per cell. The left wall remained stationary, while the right wall had a sinusoidal velocity profile, as shown in Figure 5.

The period of oscillation (t_{osc}) was 5 ms. The gas was Argon, and the numerical conditions are shown in Table 3. To evaluate both NTC and MCF, we varied the timestep and number of particles per cell. Two timesteps were tested: $\Delta t = \tau_{TH}/10$, and $\Delta t = \tau_{TH}$. Although 20 particles per cell is the rule of thumb for DSMC simulations, that was not

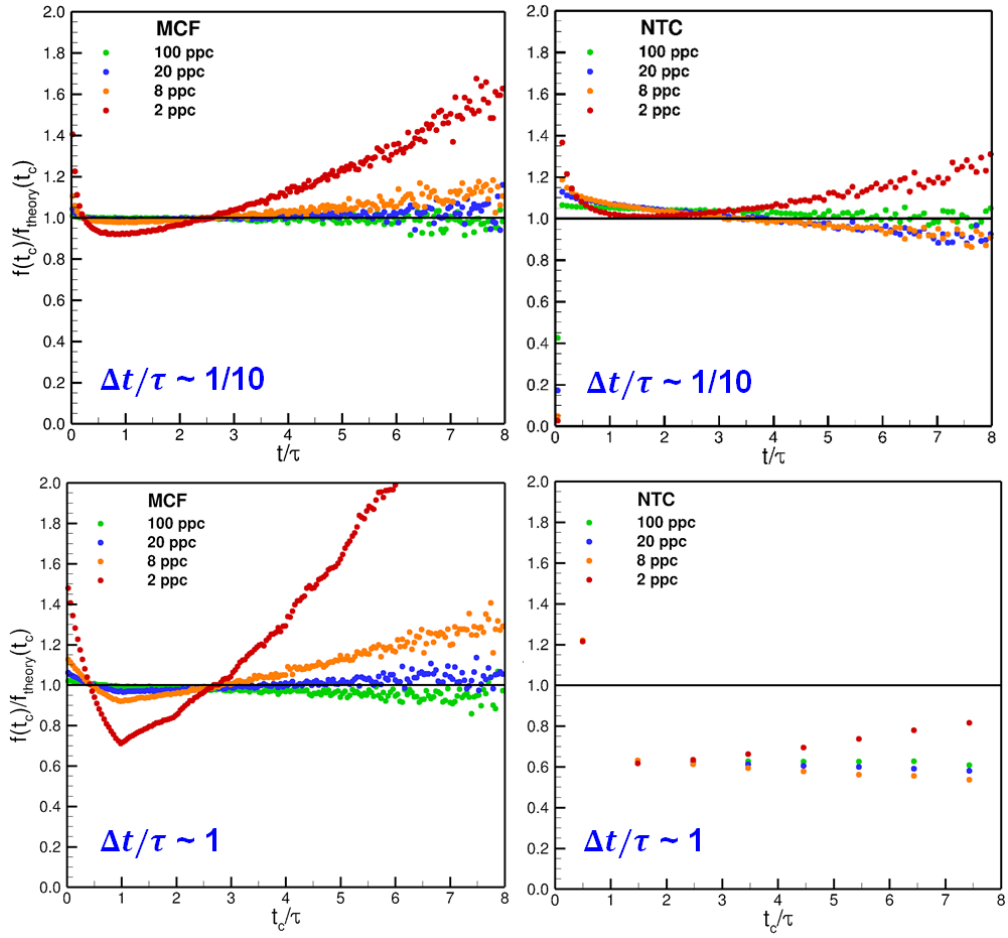

FIGURE 4. Comparison of PDF of time between collisions for NTC and MCF with a varrying timestep and number of particles per cell. MCF reproduces the PDF well, even with a large timestep.

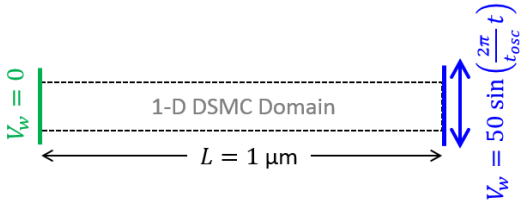

FIGURE 5. Boundary conditions for 1D Oscillatory Couette flow case

sufficient here. As previously verified [10], one needs at least 1,000 particles per cell to obtain present solutions with an acceptable level of statistical scatter. The two cases for particles per cell tested were 1,000 and 10,000.

For all test cases, we wanted to keep the same sample size, meaning for the smaller timestep ($\tau_{TH}/10$), we had less particles per cell (1,000), and for the larger timestep (τ_{TH}), we had more particles per cell (10,000). However, we needed a reference case to compare the solutions to. The reference solution was the case with the most samples: the smaller timestep ($\tau_{TH}/10$) with more particles per cell (10,000). With this being a Couette flow, the solution of interest was the velocity profile. The results are shown in Figure 6. We can see that both the MCF and NTC solutions appear very similar for all cases. For a set of timestep and number of particles/cell, both NTC and MCF capture the same

TABLE 3. Investigated numerical and VHS conditions for unsteady couette flow

n [m^{-3}]	1.68x10^{20}
T [K]	273
m [kg]	6.634x10^{-26}
t_{osc} [ms]	5
Δx_{cell} [μm]	
$Fnum$	6.72x10^{9}
τ_{TH} [μs]	2.09
T_{ref} [K]	273
d_{ref} [m]	4.11x10^{-10}
ω [-]	0.81
α [-]	1.4

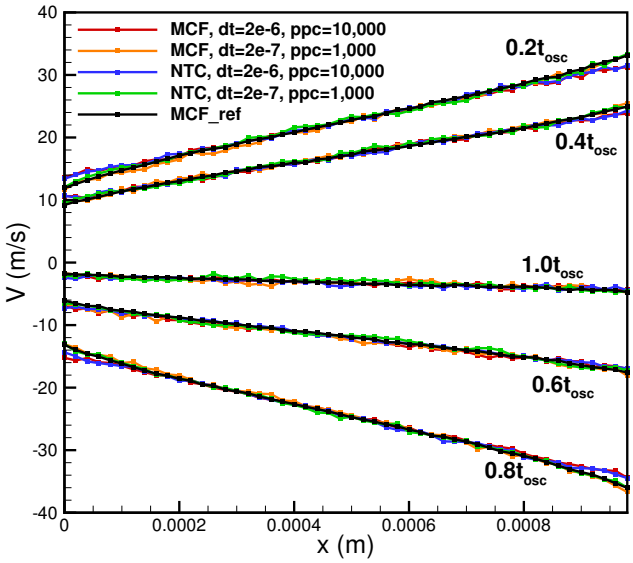

FIGURE 6. Velocity profiles for unsteady Couette flow case. Both MCF and NTC have similar results.

evolution of the velocity profile. Neither scheme seems beneficial here.

2D Compression Flow

Comparing MCF and NTC in a nonreacting hypersonic (Mach 10) flow around a circle is of interest due to the compressive nature of the flow in the shockwave. The numerical conditions are shown in Table 4, where X and Y are the dimensions of the domain. Three cases were run with different timesteps: $\Delta t/\tau_{TH} \sim 1/500$, $\Delta t/\tau_{TH} \sim 1/10$, and $\Delta t/\tau_{TH} \sim 1$. The Knudsen number was 0.3. The freestream consisted of only N_2 with a velocity of 3526 m/s. The results are shown in Figure 7. It is clear that even for unrealistic timesteps, the flowfields for MCF and NTC look nearly identical. The force results are also shown in Table 5. There are differences in the forces for different timesteps, but they are nearly identical when comparing MCF and NTC for the same timestep. For this case, NTC ran about 15% faster than MCF, but that difference could be due to innefficiencies in the MCF implementations.

TABLE 4. Investigated numerical and VHS conditions for 2D flow around a circle

n [m^{-3}]	1.0x10^{20}
X [m]	1
Y [m]	0.5
T [K]	300
m [kg]	4.65x10^{-26}
Δx_{cell} [mm]	1
$Fnum$	1x10^{14}
τ_{TH} [μs]	5.0x10^{-5}
T_{ref} [K]	273
d_{ref} [m]	4.07x10^{-10}
ω [-]	0.74
α [-]	1.6

TABLE 5. Force results in the x-direction for all cases

	NTC	MCF
$\tau_{TH} \sim 1$	2.769	2.770
$\tau_{TH} \sim 1/10$	2.409	2.413
$\tau_{TH} \sim 1/500$	2.367	2.366

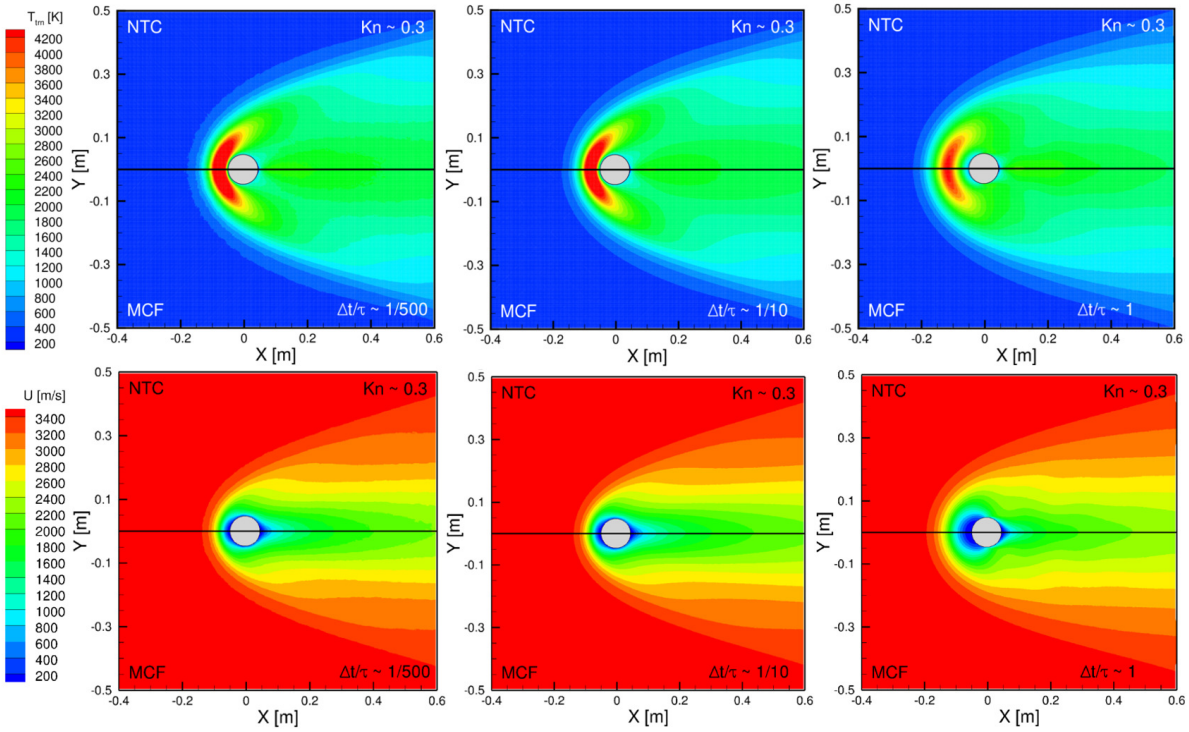

FIGURE 7. Hypersonic flow over a cylinder: Temperature and Velocity flowfields. Both MCF and NTC produce nearly identical flowfields.

2D Expansion Flow

The last case of interest was a expanding plume problem. This case was of interest as the flow density can vary by orders of magnitude. The gas composition was 96% He and 4% N_2O. The stagnation pressure is 500 mbar, and the

channel opening was 0.25 mm, meaning the Knudsen number is $5.85\text{x}10^{-6}$. The number density flowfield is shown in Figure 8. The original hypothesis was with the rapid variation in density, MCF and NTC would show differences in regions of low density. However, the results are nearly identical.

TABLE 6. Investigated numerical and VHS conditions for expanding plume flow

n [m^{-3}]	$2.91\text{x}10^{27}$	Δt [s]	$1\text{x}10^{-11}$
X [mm]	25	T_{ref} [K]	273
Y [mm]	25.025	$d_{ref,N2O}$ [m]	$5.56\text{x}10^{-10}$
T [K]	298	$d_{ref,He}$ [m]	$2.30\text{x}10^{-10}$
m_{N2O} [kg]	$7.31\text{x}10^{-26}$	ω_{N2O} [-]	0.94
m_{He} [kg]	$0.665\text{x}10^{-26}$	ω_{He} [-]	0.66
Δx_{cell} [μm]	25	α_{N2O} [-]	1.57
Fnum	$1.8\text{x}10^{17}$	α_{He} [-]	1.35
n [m^{-3}]	$2.91\text{x}10^{27}$	Δt [s]	$1\text{x}10^{-11}$
X [mm]	25	T_{ref} [K]	273
Y [mm]	25.025	$d_{ref,N2O}$ [m]	$5.56\text{x}10^{-10}$
T [K]	298	$d_{ref,He}$ [m]	$2.30\text{x}10^{-10}$
m_{N2O} [kg]	$7.31\text{x}10^{-26}$	ω_{N2O} [-]	0.94
m_{He} [kg]	$0.665\text{x}10^{-26}$	ω_{He} [-]	0.66
Δx_{cell} [μm]	25	α_{N2O} [-]	1.57
Fnum	$1.8\text{x}10^{17}$	α_{He} [-]	1.35

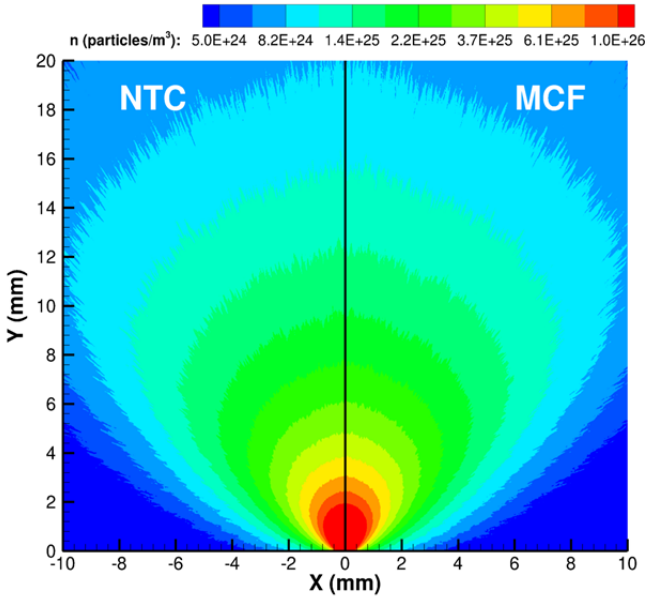

FIGURE 8. Expansion flow: number density flowfield. Both schemes produce similar results.

CONCLUDING REMARKS

Majorant collision frequency was implemented in DSMC-SPARTA. The 0-D test cases showed that although both NTC and MCF reproduce the mean collision frequency, NTC does not reproduce the Poisson distribution for time between collisions very well. MCF, on the other hand, can reproduce Poisson distribution well, even for unrealistically

large DSMC timesteps. Despite this, there appears to be no application where MCF is computationally beneficial, as the three considered benchmark cases revealed no apparent differences. The question still remains, is there a case where reproducing the mean collision frequency is not sufficient, and one needs to reproduce the Poisson distribution of time between collisions? This work can be extended to look at reactive problems.

REFERENCES

[1] G. A. Bird, *Molecular Gas Dynamics and the Direct Simulation of Gas Flows* (Oxford University Press, New York, 1994).

[2] W. G. Vincenti and C. H. Kruger, *Introduction to physical gas dynamics*, Vol. 246 (Wiley New York, 1965).

[3] M. Ivanov and S. Rogasinsky, Russian Journal of numerical analysis and mathematical modelling **3**, 453–466 (1988).

[4] M. A. Gallis, J. R. Torczynski, S. J. Plimpton, D. J. Rader, and T. Koehler, "Direct simulation monte carlo: The quest for speed," in *AIP Conference Proceedings*, Vol. 1628 (AIP, 2014), pp. 27–36.

[5] M. Ivanov, A. Kashkovsky, S. Gimelshein, G. Markelov, A. Alexeenko, Y. A. Bondar, G. Zhukova, S. Nikiforov, and P. Vaschenkov, "Smile system for 2d/3d dsmc computations," in *Proceedings of 25th International Symposium on Rarefied Gas Dynamics, St. Petersburg, Russia* (2006), pp. 21–28.

[6] A. Venkattraman, A. A. Alexeenko, M. Gallis, and M. Ivanov, "A comparative study of no-time-counter and majorant collision frequency numerical schemes in dsmc," in *AIP Conference Proceedings*, Vol. 1501 (AIP, 2012), pp. 489–495.

[7] G. Bird, Journal of Fluid Mechanics **30**, 479–487 (1967).

[8] K. Koura, The Physics of fluids **29**, 3509–3511 (1986).

[9] T. Abe, NASA STI/Recon Technical Report N **95** (1994).

[10] S. Jaiswal, A. A. Alexeenko, and J. Hu, arXiv preprint arXiv:1809.10186 (2018).